Volume 1 | Number 1 | Jan 2013 | Pages 1–100

Green Chemistry

Cutting-edge research for a greener sustainable future

www.rsc.org/greenchem

Stille couplings in water @RT

ROYAL SOCIETY OF CHEMISTRY

ROYAL SOCIETY OF CHEMISTRY

www.rsc.org/greenchem

Journal Name

Green Chemistry

ARTICLE TYPE

Efficient and Stable Star-Shaped Plasticizer for Starch: Cyclic Phosphazene with Hydrogen Bonding Aminoethoxy Ethanol Side Chains

5 **Virginia P. Silva Nykänen*[a,b], Outi Härkönen [a], Antti Nykänen [a,b], Panu Hiekkataipale[a], Janne Ruokolainen[a] and Olli Ikkaka[a]**

Starch is a sustainable polysaccharide with major existing and foreseen applications. Even if a plethora of
10 routes have been described to plasticize it, eg. by glycerol, sorbitol, and polyols, there remain major
challenges related to retrodegradation, stability, and plasticizer leaching. Here we describe plasticization
of starch using star-shaped molecules to combine the seemingly conflicting requirements: efficient
plasticization typically assigned to low molecular weight hydrogen bonding plasticizers and reduced
leaching typical for high molecular weight molecules. The efficient plasticization is allowed by the short,
15 flexible, and hydrogen bonding dangling side chains, which are connected to the core of the plasticizer,
leaving crystalline starch domains to allow self-reinforcement. The star-shaped plasticizer, a cyclic
phosphazene having six covalently bound aminoethoxy ethanol side groups was synthesized via
nucleophilic substitution, and a series of films using rice starch and different weight fractions of
plasticizer were prepared by drop casting. Incorporating ≥ ca. 10 wt% of plasticizer leads to transparent
20 plasticized films. FTIR indicates that the samples having ≤ ca. 60 wt% of plasticizer involve both
plasticized amorphous domains and reinforcing crystalline domains, suggesting self-reinforced
nanocomposite structures. The composition with 20 wt% of plasticizer shows high tensile modulus of
1.12 GPa and yield strength of 20.9 MPa, still showing a large strain of 8.8%. No retrodegradation is
observed after two months and no clear tackiness is observed even during aging of one year, suggesting
25 stability and suppressed plasticizer leaching. We suggest that the star-shaped hydrogen bonding
plasticizers allow promising potential to optimize starch-based materials for advanced applications.

.

Introduction

Starch is a widely available natural polysaccharide, which is the
30 main component of plant tubers and endosperm seeds.[1-5] It has
attracted extensive technological attention because of its
sustainability, low cost, and renewability, as well as being easy to
extract, purify, process, and scale-up. Starch has major
applications in food industry, packaging, adhesives, paper, and
35 biocomposites.[6-13] Due to its biocompatibility, starch has also
been extensively explored for biomedical purposes such as drug
delivery, tissue engineering, and wound-dressing. However,
starch is brittle, requiring chemical or physical modification for
mechanically demanding applications, and to allow film
40 formation.[14-18]

Starch is composed mainly of two kinds of polysaccharides,
namely amylose and amylopectin.[2,5] Amylose is essentially a
linear polymer formed by D-glucose units linked via α-(1→4)

bonds, with molecular weight in the order of 10^5 - 10^6 Da. By
45 contrast, amylopectin is a highly branched and high molecular
weight polymer (10^7 - 10^9 Da), formed also by D-glucose units
linked via α-(1→4) bonds, with branching points formed of α-
(1→6) glucosidic links, which are localized ca. every 20 - 70
glucose units. Starch forms granules, which consist of concentric
50 amorphous and crystalline lamellar growth rings. The crystalline
growth rings are composed of amylopectin chains in a double
helix conformation as laterally tightly packed, forming
nanoscopic crystalline layers, as separated nanoscopic amorphous
layers of amylose and the branches of amylopectin. The
55 amorphous layers are located around the branching nodes of
amylopectin.[2,5,19-21]

The classical processing of starch starts by the destruction of the
crystalline parts by heat and water treatment, in a phenomenon
called gelatinization, where the water acts as a plasticizer. In this
60 process, the highly organized granular structure is destroyed,

Green Chemistry Accepted Manuscript

most of the intermolecular hydrogen bonds are suppressed, and the starch polymer chains swell producing a viscous solution, i.e., the thermoplastic starch (TPS) that can be processed using traditional plastic processing techniques.[6,20-22,23] However, the films prepared solely using water gelatinization tend to undergo retrodegradation, where amylopectin is partly recrystallized and material becomes brittle due to insufficient segmental mobility in the amorphous domains.

To plasticize towards temporally stable thermoplastic behavior and film formation ability, organic plasticizers such as glycerol, oligoethyleneglycols, sorbitol, urea, sugars, amides, ethanolamine, citric acid, or their combinations are classically used.[6,22,24-32] Selection of proper plasticizers is critical, relevant, and subtle, aiming to promote the polymer chain dynamics under mechanical deformations, where molecularly compatible low molecular weight compounds are usually most effective.[33,34] However, a generic feature of low molecular weight plasticizers is that they are prone to migration and leaching from polymers, causing surface tackiness and lack of temporal stability.[33,35] In general, the migration can be reduced by increasing the molecular weight of the plasticizer and even using polymers, but such molecules can be less effective in plasticization. A desirable starch plasticizer should show suppressed migration and lead to diminished water absorption, as well as being biodegradable to keep the end product bio-friendly, and to lead to the increased chain dynamics allowed by the low molecular weight plasticizers[35-37].

In general, as hydrogen bonds are characteristic in starch, it is expected that also the plasticizer should be able to form extensive hydrogen bonds with starch, similarly as the classical polyols plasticizers.[38]

Here our hypothesis is that the above competing starch plasticizer requirements could be approached by using star-shaped architecture, having increased molecular weight of the whole molecule to suppress the migration and leaching, but incorporating short mobile and dynamic hydrogen bonding polyol dangling side chains for plasticization. In fact, in a different field related to ionic conductors, a slightly related plasticization concept has turned out to be feasible.[39] Cyclophosphazenes are inorganic rings containing alternating phosphorus and nitrogen atoms, and the most common cyclophosphazene is hexachlorocyclotriphosphazene $(NPCl_2)_3$, i.e., HCCP. It can be synthesized from PCl_5 and NH_4Cl, and it is also commercially available.[40]

It can be easily functionalized by replacing the chlorine atoms by appropriate organic groups. In principle, any nucleophile can be introduced to the phosphazene ring via nucleophilic substitution reaction. Some features that are intrinsic to phosphazene rings are flame resistance, thermal stability, and degradation into non-hazardous molecules, i.e., phosphates and ammonia. However, it is important to notice that the non-hazardousness is also dependent on the type of the organic group attached to the phosphazene ring.[40-44]

As six chlorine atoms are linked to phosphorus in HCCP, six nucleophiles can be introduced in the ring producing a multifunctional molecule that can hold, for example, six flexible polyol chains.

Motivated by this idea, we synthesized star-shaped cyclophosphazene molecules bearing aminoethoxy ethanol side groups, and prepared a series of phosphazene/starch mixtures. Their properties were investigated by spectroscopies, small angle X-ray scattering, electron microscopy, and mechanical studies.

Experimental

General procedures

Hexachlorocyclotriphosphazene (99%, Aldrich) was purified by re-crystallization from hexane at 50 ^{o}C followed by sublimation at 55 ^{o}C under low pressure (2.8 x10^{-3} mbar) using a cold finger apparatus. 2-(2-Aminoethoxy) ethanol, i.e. AEE, (98%, Aldrich) was treated with CaO and stored under molecular sieves (4 Å). Tetrahydrofuran was treated with potassium and benzophenone over reflux before use. The synthesis was carried out under dry nitrogen using standard Schlenk line techniques. Rice starch (Aldrich) was used as received; deionized water was used for gelatinization of starch and homogenization of the mixtures.

Synthesis of aminoethoxy ethanol substituted phosphazene - $N_3P_3(C_4H_{10}NO_2)_6$ - AEEP

1.0 g (2.9 mmol) of hexachlorocyclotriphosphazene was dissolved in approximately 500 mL of THF and added dropwise to a stirring solution containing 3.6 g (35 mmol) of 2-(2-aminoethoxy) ethanol and 20 mL of triethylamine dissolved in 300 mL of THF. The reaction was conducted in dilute conditions to avoid or minimize cross-linking side reactions between the rings. Triethylamine was used as hydrochloric acid scavenger. The reaction mixture was stirred at room temperature for 12 hours and at 40 ^{o}C for another 12 hours. The reaction was finished by cooling down the mixture to room temperature. The resulting material, which was precipitated in the reaction flask, was separated from the THF solution and washed with a solution of THF/methanol (5:1). Thereafter, the paste was dissolved in a small amount of ethanol and precipitated first against THF and then, against hexane several times. The final product, a sticky and pale yellow paste, was obtained by evaporating the solvent in a rotary evaporator. NMR ^{31}P (600 MHz, D$_2$O, ppm): 20.8 (d); 23.6 (t) ($J = 51$ Hz). ^{1}H (600 MHz, DMSO, ppm): 3.01 (m, br, NH$_2$-CH_2-); 3.12 (t, -NH-CH_2-); 3.52 (t, -P-O-CH_2-); 3.55 (t, -O-CH_2-CH$_2$-OH); 3.58 (t, -O-CH_2-CH$_2$-O-P-); 3.60 (m, -O-CH_2-CH$_2$-NH$_2$); 3.67 (t, -O-CH_2-CH$_2$-NH-); 3.70 (t, HO-CH_2-CH$_2$-). FTIR (cm^{-1}): 3255 (-OHν); 2870 (-CH$_2$ νsym.); 1609 (N-H δscissor); 1504 (N-H wagging); 1270 (N-P=N); 1226 (O-P=N); 1112, 1064, 960 (C-Oν and P-Oν). m/z = 760.36 (MH$^+$).

Processing of the films

We prepared 0.5 g starch/AEEP mixtures with the following AEEP dry mass concentrations: 10, 20, 30, 40, 50, 60, 70, 80, 90 wt%. The reference sample without AEEP was prepared using only starch and water. Starch was added at room temperature into a beaker containing a large excess of deionized water, leading to the starch concentration < 15 wt%. The mixtures were heated up to 95 ^{o}C under vigorous stirring. After 10 minutes, the mixtures became clear, and the phosphazene plasticizer (as dissolved in a
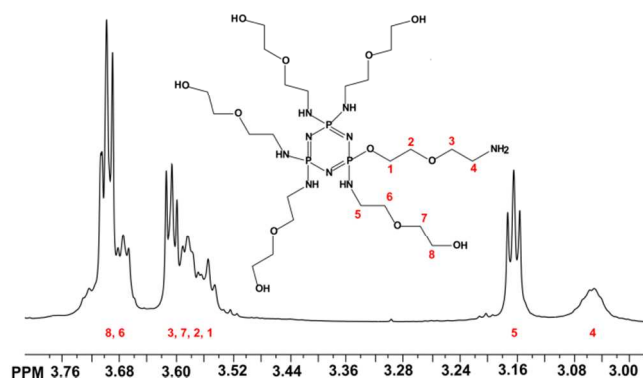
Fig. 1 Suggested structure for AEEP as well as the ^{1}H NMR spectra (D$_2$O, 600 MHz).

minimum amount of water ~5 mL) was added dropwise into the starch/water slurry. The mixtures were further stirred at 90 °C until the volume decrease to about half of the initial volume. After that, the mixtures were cast onto Teflon dishes and taken to an oven, where the films were dried at 40 °C, under a constant air flow. The drying process took about 6 hours.

Fourier transform infrared spectroscopy (FTIR)

The spectra were recorded using a ThermoNicolet 380 spectrometer and ATR method (diamond crystal). The spectra were collected from both fresh dried samples and samples stored for 60 days at room temperature and 37-40% relative humidity.

Nuclear magnetic resonance spectroscopy (NMR)

The ^{1}H and ^{31}P spectra were acquired in an equipment Varian Inova 600 MHz using Si(CH$_3$)$_4$ as internal reference for ^{1}H experiments and H$_3$PO$_4$ in an external capillary reference as for the ^{31}P experiments, all recorded at 27 °C.

Differential scanning calorimetry (DSC)

The measurements were carried out on a Mettler Star DSC 821 at heating rates of 10 °C·min^{-1}. The samples (~5 mg) were placed in an aluminum pan and heated up to 100 °C under N$_2$ atmosphere in a first scan, followed by a cooling stage until -20 °C. A second scan was carried out by heating up to 250 °C at the same heating rates. The second scan was used to quote the thermal events.

Mechanical tensile testing

The tensile tests were carried out on a DEBEN minitester (Microtest 200 module) equipped with a 20 N load cell. Measurements were conducted at room temperature (22 ± 1 °C) and 37% relative humidity level. The sample films were kept under such conditions for two days before the measurements. The films were cut in rectangular shapes of 20 mm x 3.0 mm, and the thickness was 60-105 μm, as measured with a Mitutoyo LGF-

0110L linear gauge. The average thickness was obtained by measuring the thickness from three different points of the specimen. 4-5 specimens were analysed for each sample. Pure starch/water was too brittle to be measured.

Thermogravimetric analysis (TGA)

The measurements were carried out on a Mettler M3-TG50, using an aluminum pan, under N$_2$ atmosphere, and heating up to 600 °C with heating rates of 10 °C·min^{-1}. To verify the water contents, the samples were conditioned under 65% relative air humidity for one week. The samples were cut in similar shapes and approximately the same weight (~3 mg) and heated up to 130 °C, followed by an isotherm stage of two hours.

Small angle x-ray scattering (SAXS)

The samples were sealed to a holder between two Kapton films to yield a sample with a thickness of approximately 60-105 μm. The structural periodicities were measured by using a rotating anode Bruker Microstar microfocus X-ray source (Cu Ka radiation, λ = 1.54 Å) with Montel Optics. The beam was further collimated with four sets of slits (JJ-X-ray), resulting in a beam size of approximately 1 × 1 mm at the sample position. The distances between the sample and the Bruker AXS 2D area detector were 1.59 m and 4.5 m. One-dimensional SAXS data were obtained by azimuthally averaging the 2D scattering data. The magnitude of the scattering vector is given by $q = (4\pi/\lambda) \sin \theta$, where 2θ is the scattering angle. The collected data was corrected for background scattering and background noise.

Scanning electron microscopy (SEM)

Field-emission scanning electron microscopy (JEOL JSM-7500FA) was performed at 2 keV electron energy. All the samples, except 10 wt% AEEP, were submerged in liquid nitrogen and broken to analyze the cross-sectional surface. The samples were sputtered with a thin layer of gold (Emitech K950X/K350, 30 mA, 45 seconds) to promote conductivity.

Results and Discussion

The star-shaped phosphazene plasticizer AEEP (Figure 1) is a transparent pale yellow and hygroscopic paste. It is soluble e.g. in water, ethanol, methanol, 1-butanol, but insoluble in THF, diethyl ether, ethyl acetate acetone and hydrocarbons. Mass spectroscopy renders the molecular weight MH$^+$ 760.36, thus agreeing with the expected chemical formula (see Figure S1 and Table S1). Figure 1 depicts the ^{1}H NMR spectrum, showing that the plasticizer indeed contains the aminoethoxy ethanol side chains. In the ^{31}P NMR spectrum, the absence of signals attributed to -PCl$_2$- or -PClR- indicates the complete replacement of chlorine atoms in the molecular substitution (see Figure S2).[45] ^{31}P NMR presented two groups of signals: the first at 20.8 ppm is attributed to the phosphorus atoms linked to two nitrogen atoms, and the second at 23.5 ppm is attributed to the phosphorus atoms linked both to the nitrogen and oxygen atoms. We could not find signals indicating phosphorus atoms linked only to two oxygen atoms. The analysis

ARTICLE TYPE
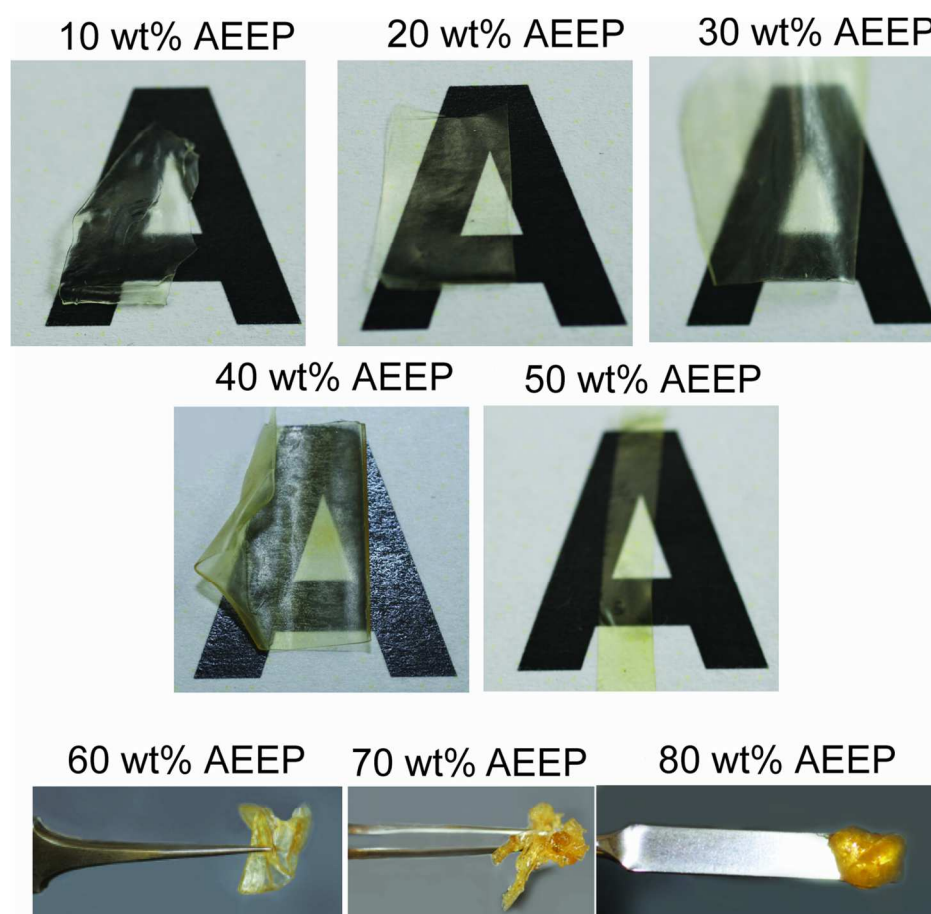
Fig. 2 Photographs of starch/AEEP compositions, showing their consistency and transparency.

Table 1 Appearance of the cast starch/AEEP composition after water evaporation.

Contents of AEEP (wt%)	Film characteristics
0	Very brittle
10	Transparent film, with some flexibility
20	Transparent film, foldable
30	Transparent film, flexible, plastic-like
40	Transparent film, flexible, soft
50	Transparent film, flexible, soft, slightly adhesive
60	Transparent, rubber-like, adhesive, difficult to peel off
70	Transparent, very soft film, adhesive
80	Transparent paste, adhesive, does not form self-standing film
90	Transparent paste, adhesive, does not form self-standing film

of ^{31}P NMR peak heights suggested that, in the average, one phosphorus at the ring underwent a substitution having nitrogen and oxygen linked, whereas the other two phosphorus atoms where substituted only via amines. This may not become as a surprise as also other works show a regioselectivity in the macromolecular substitution of bifunctional nucleophilies, with preferred substitution via amine rather than alcoholic hydroxyl.[46-49]

In fact, the above suggested statistical mixture of both reaction topographies may even be favorable to promote plasticization, as suppression of regularity is attractive for suppressed crystallization and efficient plasticization. Also, whether the aminoethoxy ethanol NH_2-$(CH_2)_2$-O-$(CH_2)_2$-OH reacts onto phosphazene ring from its amine or hydroxyl group, the opposite peripheral hydroxyl or amine end groups can still allow hydrogen bonding to starch. Figure 1 shows a suggested statistically averaged structure for AEEP.

The bifunctionality of aminoethoxy ethanol could, in principle, also lead to a cross-linking of the phosphazenes to form an insoluble cyclomatrix, if the same aminoethoxy ethanol molecule

ARTICLE TYPE
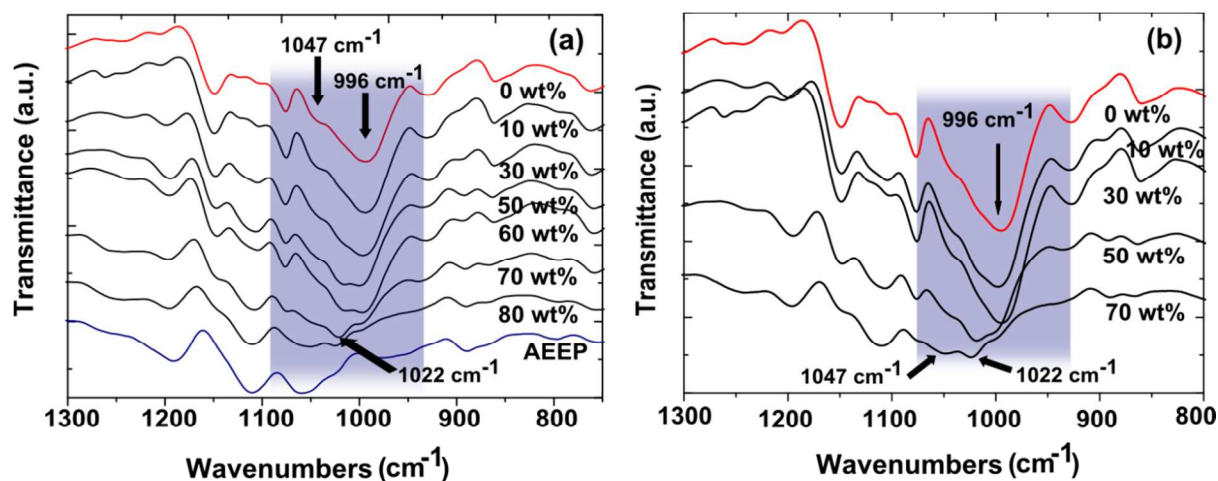
Fig. 3 FTIR-ATR spectra of selected starch/AEEP films (see all spectra in Figure S3). (a) Freshly dried sample and (b) sample after aging of 60 days under 37 - 40% humidity. The shaded region shows the bands attributed the crystalline and amorphous domains of starch. The labels indicate fraction of AEEP.

5

reacts with two neighbouring rings through its two reactive sites. However, no evidence for the cyclomatrix formation was observed by mass spectroscopy, which does not come as a surprise as the reaction was carried out in very dilute conditions. 10 Moreover, the material remained soluble after long periods of time, even when exposed to atmosphere. The fact that the substitution reaction can be carried out without the help of protection/deprotection techniques is relevant, because it simplifies the reaction procedures, reducing the formation of the 15 residues and the costs.

Structural and morphological characterizations of the starch/AEEP films

The cast films are shown in Figure 2 and their properties are 20 summarized in Table 1. All the films are visually transparent and macroscopically homogeneous. At small plasticizer weight fractions up to ca. 50 wt% the films were robust and could be peeled away from Teflon dishes. At higher concentrations the films became gradually softer and eventually paste-like and too 25 adhesive, preventing their removal. Upon aging of ca. one year, the films kept their initial transparency and flexibility, thus suggesting stability. The transparency of the cast films gave us a first sign that starch and AEEP are intimately mixed producing a homogeneous material, at least in macroscopic scale. This is 30 untrivial, as attempts to plasticize starch films e.g. using poly(ethylene glycol) - PEG 200 (M_w 210 - 320 Da) - by drop casting lead to opaque and brittle films.[25,50] Taken our star-shaped hydrogen bonded plasticizer of relative high molecular weight, these observations indirectly indicate, that it is not only the

35 chemical composition and molecular weight that play an important role in the effectiveness of the plasticizer, but its geometrical structure is also a key factor.

FTIR

40 The films were analyzed by FTIR-ATR first soon after drying and additionally after 60 days of storage at room temperature at 37-40% relative humidity, in order to observe whether structural changes took place upon aging. Representative spectra are displayed in Figure 3, and the spectra of the whole series together 45 with a summary of the band shifts are included in Supporting Information (see Figure S3 and Table S2).

The emphasis is here in the fingerprint spectral region of polysaccharides in the bands from 1300 to 800 cm^{-1}. Three bands are investigated in detail: the band close to 1000 cm^{-1}, which is 50 assigned to the hydrated crystalline structure of amylopectin, and is related to the hydrogen bonding of the hydroxyl group at C-6.[51] The band at 1047 cm^{-1}, which consists of overlapping bands of 1040 and 1053 cm^{-1}, is related to the aligned double helices (see later Figure 6), and the band at 1022 cm^{-1}, is attributed to the 55 amorphous parts of starch.[52]

A major absorption band is observed at ca. 996 cm^{-1} for AEEP concentrations up to ca. 60 wt%, which is related to the crystalline starch domains. For higher AEEP concentration only a shoulder is observed, whereas in pure AEEP this band is not 60 observed. Similarly, a clear shoulder at 1048 cm^{-1} is observed for AEEP concentrations below ca. 60 wt% and hardly resolved for higher concentrations. These two bands are attributed to the hydrated crystals and aligned double helices of starch. The band

1022 cm^{-1}, related to the amorphous domains, is not resolvable in lower concentrations of AEEP, becoming distinct at 70 wt% AEEP. Note that 50 and 60 wt% as well as pure AEEP have a small absorption near this same band, but in the sample containing 70 wt% the absorption at 1022 cm^{-1} was particularly more intense. One can conclude that in starch/AEEP mixtures there are coexistent crystalline and amorphous starch domains up to ca. 60 wt% AEEP plasticizer. Clear indications of rupture of the crystalline structure were only detected at 70 wt% or higher plasticizer concentrations.

Figure 3b depicts selected FTIR spectra upon aging for 60 days.
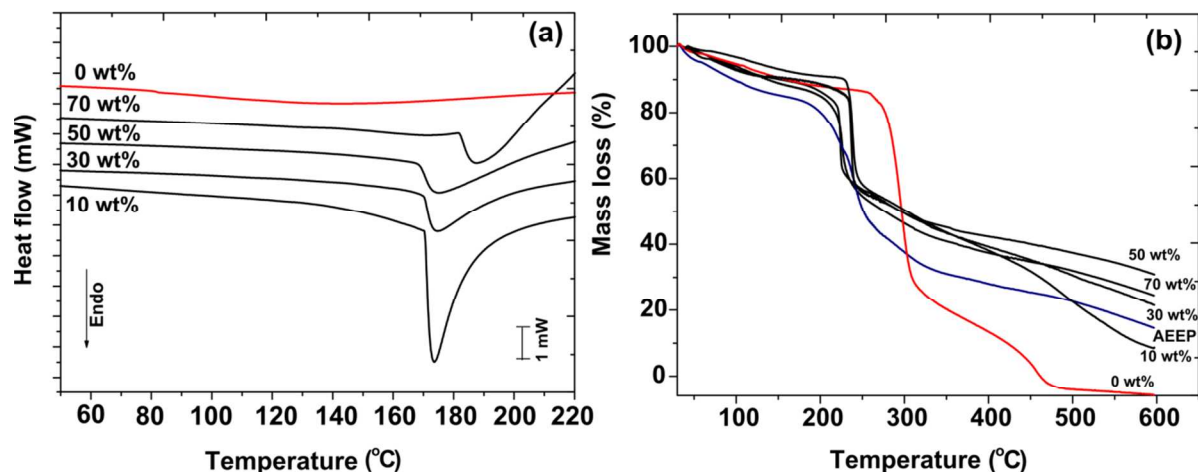
Fig. 4 (a) DSC curves of selected samples in the region of T_m at the heating rates 10 ^{o}C·min^{-1}, (b) TGA curves of selected samples. The labels indicate fraction of AEEP.

The bands close to 996 cm^{-1} and 1048 cm^{-1}, related to the crystalline domains, are observed even at the high 70 wt% concentration of the plasticizer, even though a small shift of the first band to higher wavenumbers may be observable. Simultaneously, the band related to amorphous structure is also observable close to 1022 cm^{-1}. As the FTIR spectra were essentially similar for the fresh and aged samples, no observable retrodegradation had taken place within these compositions during the 60 days and under 37-40 % relative humidity, which indicates sample stability.

The FTIR results suggest that there are both crystalline and amorphous domains within the starch/AEEP composition for any practically relevant compositions, i.e. where the weight fraction of AEEP is not excessive.

Thermal characterization

The DSC experiments (Figure 4a, Table 1 and Figure S4) showed a single endothermic peak for the compositions up to 70 wt% of AEEP, which was attributed to the melting of starch crystals. The T_m varied from 158 to 178 ^{o}C, and for the concentration of 70 wt% AEEP, T_m shifted to a higher temperature. The samples containing 80 and 90 wt% also showed endothermic peaks, but they are not shown in Figure 4 due to the proximity of their degradation process, which started at 219 and 220 ^{o}C, respectively. Thus, the data of those samples were not reliable enough to be used in the quantitative analysis. The T_m values found for these films are consistent with the melting temperature calculated for a perfect starch crystal, which varies from 160 to 200 ^{o}C, depending on the starch source.[56] However, the present temperatures are slightly higher than the ones reported for films composed of starch and its most common plasticizers.[25] Pure starch films prepared from water did not present endothermic peaks in the range of analysed temperatures. The high enthalpy value indicates that the addition of 10 wt% AEEP probably induces a particularly stable crystalline structure, which requires higher energy for melting.

The glass transition temperature (T_g) found for the pure AEEP was -39.9 ^{o}C. The starch/AEEP samples presented a single T_g up to 60 wt% of AEEP. The values of the T_g decrease until reaching a minimum of -24.3 ^{o}C for the sample containing 50 wt% AEEP. However, at high concentrations of AEEP, such as at 70 wt% or beyond, the observations become less clear, even pointing towards phase separation. In any case, such AEEP concentrations are not practical.

TGA for the studied starch/AEEP mixtures showed only one major degradation step near 230 ^{o}C within the interval of temperatures analysed, see Figure 4b and Figure S5. Films containing 10, 80 and 90 wt% AEEP, and the pure starch/water sample presented an additional degradation step. In all cases, the values of the decomposition temperatures of the first step ($T_{d,1}$) were lower than $T_{d,1}$ of pure components. As a general feature, we observed that $T_{d,1}$ slightly decreased with the increase of the amount of AEEP. This was especially true for the samples with 20-90 wt% AEEP. The presence of a single degradation step suggested strong interactions between starch and plasticizer, which was very likely entrapped within the starch structure. The behavior of the film containing 10 wt% AEEP was markedly different from the other samples, being more similar to starch/water sample with respect to the number of decomposition

Journal Name

Green Chemistry

ARTICLE TYPE

Table 2 TGA and DSC data for dried AEEP/starch mixtures.

Contents of AEEP (wt%)	TGA				DSC		
	$T_{d,1}$ (°C)	$T_{d,2}$ (°C)	Char (%)	Water absorbed (%)*	T_m (°C)	Enthalpy (J.g^{-1})	T_g (°C)
0	297	457	0	11.0	-	-	-
10	238	504	8.5	9.2	173	59.2	-13.6
20	231	-	16.4	10.1	171	41.0	-17.2
30	226	-	20.5	10.4	174	46.8	-20.3
40	226	-	23.7	11.9	158	50.8	-22.4
50	224	-	30.9	12.6	174	40.6	-24.3
60	223	-	26.4	13.8	178	29.8	-18.3
70	225	-	24.6	14.8	187	20.5	-8.7 / -45.8
80	219	249	17.4	18.3	-	-	-
90	220	239	14.6	22.8	-	-	-
100	255	-	10.3	-	-	-	-39.9

[a] Samples conditioned in a chamber at humidity level of 57-63%.
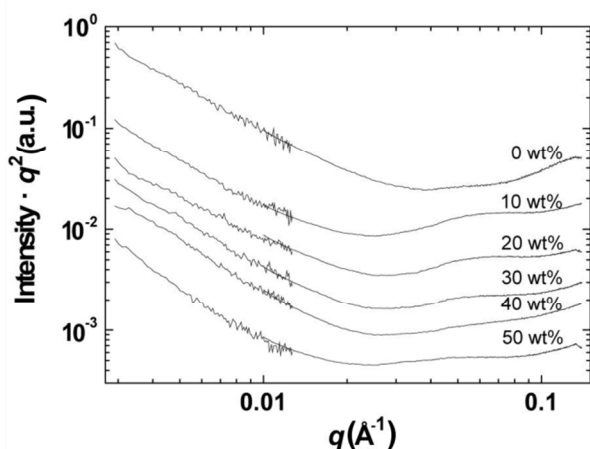
Fig. 5 SAXS intensity patterns of starch/AEEP films. The weight fractions indicate the increasing fraction of AEEP in the samples. The amount of water varied from 9.2 - 12.6 wt% according to TGA measurements (Table 2).

steps and $T_{d,2}$. An interesting feature is the difference of $T_{d,2}$ between the sample without plasticizer and the sample with 10 wt% of AEEP, the values being 457 °C and 504 °C, respectively. According to the literature, plasticized starch presents two steps of decomposition, the first relating to the amorphous parts of the starch ring, and the second to the well packed crystalline part.[16] These values indicate that the crystals indeed prevailed after addition of 10 wt% of AEEP to the starch/water system because the sample required more energy to be decomposed, due to a more regular organization.

As the properties of starch-derived materials strongly depend on the humidity level, and in addition, as AEEP is a very hygroscopic material, we evaluated the water intake of the samples using TGA. The results showed an increase in the water intake with the amount of AEEP in the samples. The samples containing 10 - 30 wt% AEEP absorbed slightly less water than the control sample (starch/water). This behavior suggests strong interactions between starch and the plasticizer. If the hydrogen bond sites in starch are occupied by the presence of AEEP, the water intake would decrease because there would not be available sites for hydrogen bonds between water and starch or water and plasticizer. Besides, the absorption of water by the compact crystalline structure, which is already been shown to exist in our system, is relatively more difficult than the absorption by the amorphous part.

The TGA results showed, interestingly, a maximum amount of char, 30.9%, for the composition having 50 wt% of AEEP (Table 2). This behavior indicates a matching with the FTIR results because the FTIR spectra showed a change of pattern also at 50-60 wt% of AEEP in sample. Phosphazenes are well known for their thermal stability and formation of chars that involve cross-linking reactions and formation of stable phosphates. Starch, on the other hand, is completely decomposed at 600 °C producing no char as observed in Figure 4b. In spite of that, starch/AEEP films, excluding 10 wt% AEEP, produced more char than pure AEEP, which confirms the interactions between starch and AEEP. A plausible explanation for the maximum amount of char in the sample containing e.g. 50 wt% AEEP is that, according to FTIR, the starch crystals were still present at that concentration and the presence of packed crystals is a factor that contributes to the amount of char formation. According to TGA results, the sample with 50 wt% of AEEP gathered the highest possible amount of phosphazene that could be introduced in the system without completely disrupting the crystalline structure, and producing the most thermally stable product of the series. For the sample with 70 wt% of AEEP, with no influence of the crystalline structure, the amount of char decreased and the same was observed for the samples with the highest AEEP concentrations.
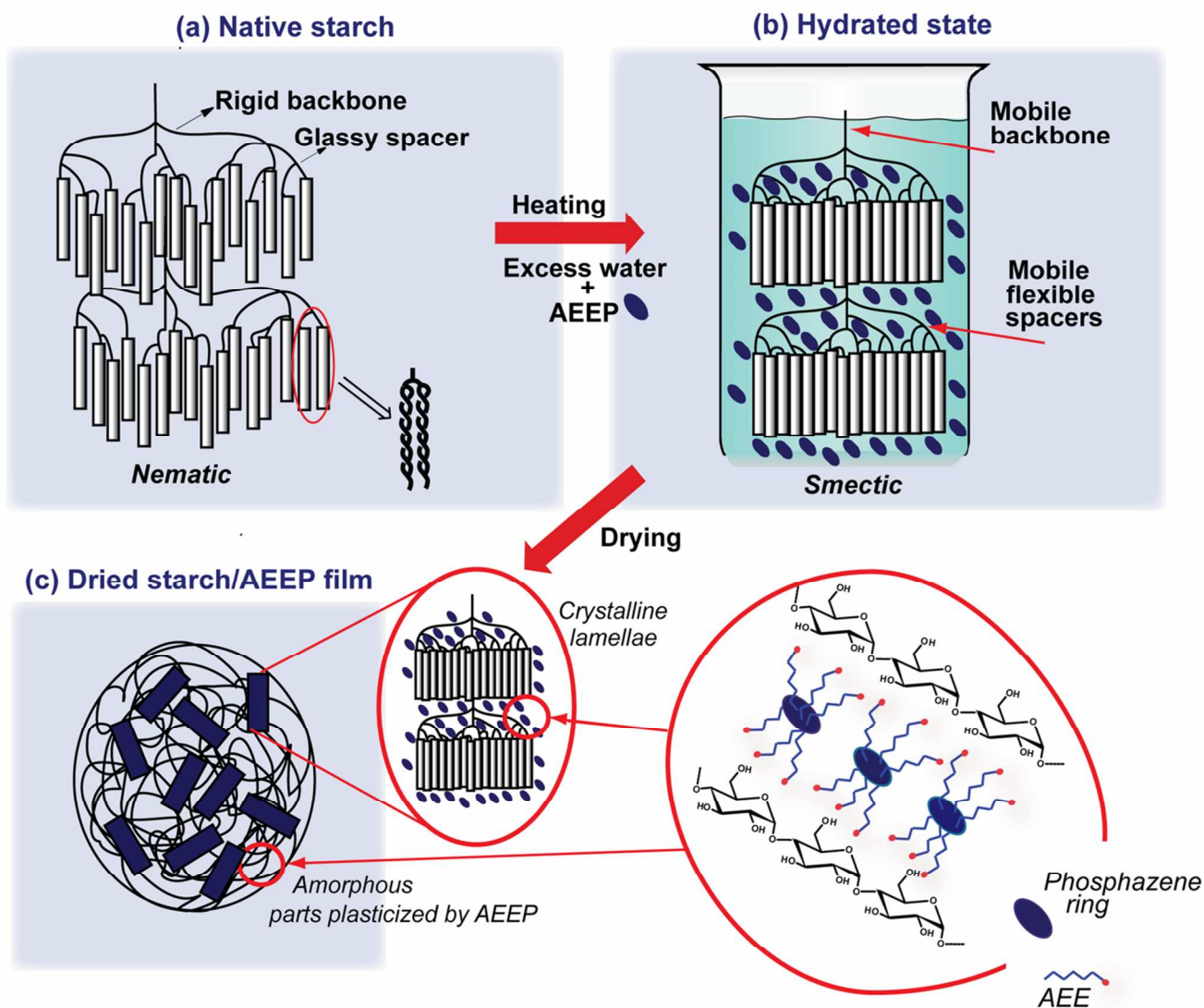
Fig. 6 Schemes for the suggested structures. (a) The native starch consisting of glassy polymer backbone and spacers and nematic array of double helices involving corrugated domain boundaries, as reported previously.[17,18,51] (b) Heating in the hydrated state is known to lead to smectic arrangements with
5 more smooth domain boundaries allowed by plasticized backbones and spacers,[17,18,51] which is expected to take place also in the case of added plasticizer AEEP. (c) The suggested structure upon drying, involving crystalline domains (based on FTIR) forming smectic arrangements and their typical periodicity (based on SAXS) allowed by plasticized spacers. The possible hydrogen bonding end group sites of the AEEP have been indicated by red dots. Note that the depicted shapes of the semicrystalline reinforcing domains could not be assigned from the SAXS or electron microscopy, and must be interpreted only schematically.

10

SAXS

Figure 5 shows the SAXS curves for starch/AEEP mixtures from dried films. For starch with no AEEP, essentially no organization is observed for the values of the scattering vector q in the range
15 0.02-0.1 Å^{-1}, corresponding to nanometer length scale. By contrast, for samples with 10 - 30 wt% AEEP concentrations, there is a broad intensity maximum observable at $q = 0.065$ Å^{-1}, which indicates structure of 9-10 nm periodicity. This periodicity has also been observed in hydrated starches, and it has been
20 assigned to the so-called smectic starch structure (see later Figure 5 for the scheme), consisting of alternating layers of crystalline lamellae of laterally packed double helices and mobile plasticized polymer backbones and spacers.[20,21,53,54] The small intensity of

the present reflection indicates poor overall order, which does not
25 come as a surprise, as rice starch generally displays especially broad scattering peaks, revealing lower degree of crystallinity than maize starch, for example.[19] At higher AEEP concentration beyond ca. 30 wt%, the SAXS peak becomes unobservable. At low magnitudes of scattering vector, the scattering shows a
30 characteristic upturn. Figure 5 shows a scaling relation $I \propto q^{-\alpha}$, where $\alpha \approx 3.5$, indicating interfacial scattering.[20] Combining the above findings with previous knowledge on starch behavior allows us to suggest potential structures. Starch can be regarded as a side-chain liquid crystalline polymer having helical side
35 chains connected to the polymer backbone via short spacers.[54] In the native form, the material is frozen to involve glassy

backbones and spacers, and the amylopectin double helices pack in a corrugated manner, denoted as nematic phase of starch, see Figure 6a.[54] The plasticization, either due to presence of solvent/plasticizer or thermal energy input will increase the

5 segmental mobility and promotes an assembly of the double helix clusters towards a smectic-like order, see Figure 6b.[19,38,54-57] The assembly obtained after hydration shows classically 9 nm periodicity in SAXS.[20] Adding AEEP is not expected to change this overall picture. The 9 nm periodicity, shown in Figure 5 for

10 the dried starch/AEEP mixtures, suggests that the smectic-like structure with crystalline and amorphous layers remains, see Figure 6c. This is supported also by FTIR results, which suggest the coexistence of the crystalline double helix packing and amorphous starch. In this model, the AEEP molecules are located

15 within the amorphous domains, promoting their segmental mobility. Taken its relatively high molecular weight, the AEEP molecules cannot easily migrate and leach, thus explaining the observed temporal stability. Still, the hydrogen bonding dangling side chains have high dynamics like small molecular plasticizers,

20 and provide efficient plasticization.[50,51]
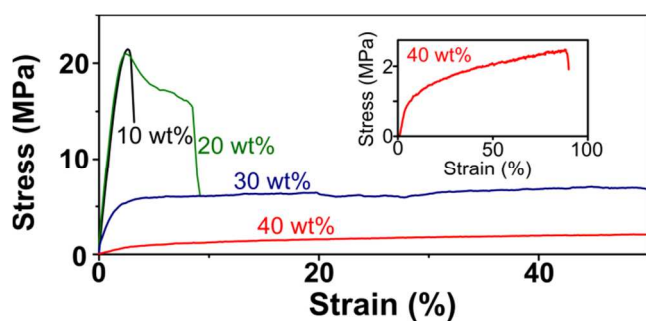
Fig. 7 Representative starch/AEEP stress-strain curves and inset showing
25   containing 40 wt% AEEP. For the complete set, see Figure S6

Tensile tests

Mechanical properties of the samples involving 10-40 wt% AEEP were recorded using a micro-tensile tester. The samples involving

30 50 - 90 wt% of AEEP were too soft and adhesive to allow peeling off robust films from the Petri dish. Starch gelatinized only with water was also not proper for tensile tests because of the brittleness. The mechanical tests were conducted approximately one week after the sample preparation. Figure 7 shows typical

35 stress-strain curves, and the mechanical properties are collected in Table 3. We comment that mechanical properties are very dependent on the preparation method, composition or processing of the films, and therefore any quantitative comparison between different films should be made with great care.

40 The mechanical properties changed markedly with the amount of AEEP. As a general feature, both the tensile strength and tensile modulus decreased with the amount of AEEP in the films. The sample containing 10 wt% of AEEP was brittle. On the other hand, elongation at break increased almost 50 times from the

45 composition involving 10 wt% of AEEP to the sample with 40 wt% of AEEP.

Table 3 Mechanical properties measured for the plasticized rice starch at room temperature and 37% relative humidity.

Weight fraction of AEEP (wt%)	Yield Strength (MPa)	Tensile Strength (MPa)	Strain at break (%)	E (MPa)	Work to fracture (J m⁻²)
10	21.4±1.3	20.6±0.8	2.2±0.3	1060±70	0.49
20	20.9±0.1	15.9±0.3	8.8±0.3	1120±80	1.51
30	4.6±0.6	5.3±0.8	47.9±8.8	270±20	0.32
40	1.5±0.2	2.32±0.14	*	20±1	0.16

50 * The micro tensile tester machine reached its maximum run with no sample breakage.

55 The work to fracture, based on the area below stress-strain curves, presented a maximum with the sample containing 20 wt% of AEEP, indicating the toughest film in this series. The distinct change in the mechanical properties as the AEEP content is increased from 20 to 30 wt% is notorious for the films becoming

60 much more ductile and soft.

The stress-strain curve of the sample having 20 wt% AEEP (Figure 7) shows regions of elastic deformation, and a pronounced plastic yield deformation. Stress strain-curve of sample with 40 wt% of AEEP also presents elastic and plastic

65 deformation, but no yield maximum. Interestingly, the previous works report that the presence of crystalline domains arising from the incomplete gelatinization of starch does not necessarily improve the mechanical properties of starch-derived materials.[53] By contrast, the present crystalline starch domains in the AEEP

70 compositions improved the mechanical properties, suggesting self-reinforced nanocomposites.[58,59]

The present starch/AEEP films display a significant improvement in comparison to the previously reported values dealing plasticized starch. Previously measured rice starch films

75 show mechanical performance of E = 530 MPa, σ = 11 MPa, ε = 3%, using 20 wt% of glycerol as a plasticizer, and E = 1050 MPa, σ = 22 MPa, ε = 3% for 20 wt% sorbitol as a plasticizer. [11,60] In another study, rice starch films show values of σ = 3.2 MPa, ε = 0.5% for 20 wt% glycerol as a plasticizer.[61] For comparison, we

80 measured E = 1120 MPa, σ = 20.9 MPa, ε = 8.8% using 20 wt% of AEEP, and even for 10 wt% AEEP E = 1060 MPa, σ = 21.4 MPa, ε = 2.2%, demonstrating its plasticizing efficiency. In fact, the values obtained for starch/AEEP films are in the same range, or even better, than the values found for starch-based polymer

85 blends, such as starch/PLA and starch/PVA, and even starch-based composites containing clay or carbon nanotubes.[67-70] A comparison between the mechanical properties of starch films plasticized with its most common plasticizers is presented in Table 4. It is important to mention that, besides mechanical

90 properties and a peculiar reinforcing mechanism, AEEP did not present leaching, which is the main problem regarding the use of common plasticizers, especially glycerol.

95

Table 4 Mechanical properties of starch films plasticized with its most common plasticizers compared with starch/AEEP film (20 wt%). *Note that different types of starch were used for this comparison.*

	Tensile Strength (MPa)	E (MPa)	Strain at break (%)	Plast. contents(%)	Ref.
starch/AEEP	**20.9**	**1120**	**8.8**	**20**	-
starch[a]/glycerol	11	530	3	20	*60*
starch[a]/glycerol	3.2	-	0.5	20	*61*
starch[b]/glycerol	5.8	97.5	36.4	40	*62*
starch[c]/glycerol	3.6	87	124	24	*63*
starch[a]/sorbitol	3.5	-	16	35	*61*
starch[a]/sorbitol	22	1050	2.8	20	*60*
starch[b]/sorbitol	5.7	106	61.2	40	*62*
starch[a]/sorbitol	10	-	5	26	*64*
starch/urea[d]	12	-	7	20	*65*
starch/formamide+urea[d]	4.6	26.8	159	30	*66*

5

[a] rice starch; [b] pea starch; [c] wheat starch; [d] corn starch;

Fracture behavior

In order to study the fracture behavior, the fractured surfaces of
10 the different samples were investigated using SEM. The images acquired from the cross-sectional area are shown in Figure 8.
. The fractured surfaces for the compositions involving 20 - 30 wt% of AEEP are uneven, indirectly suggesting energy dissipation upon fracturing.
15

Conclusion

20

Starch gelatinized by water was here plasticized using a star-shaped plasticizer based on phosphazene rings bearing flexible hydrogen bonding aminoethoxy ethanol side chains. The compositions showed coexistent crystalline reinforcing and
25 plasticized amorphous lamellae up to 60 wt% AEEP. We suggest that the star-shaped plasticizers facilitate combination of efficient plasticization, usually assigned to low molecular weight molecules, and reduced migration and leaching classically assigned to larger molecules which usually have poor
30 plasticization efficiency. No clear retrodegradation was observed by FTIR after 60 days. SAXS scattering patterns showed a broad peak indicating a periodic structure of 9-10 nm matching with the values normally found for the periodic lamellar smectic-like structure of hydrated starch systems. Stress-strain curves indicate
35 a change from brittle to soft materials with the increasing plasticizer content, showing toughest behavior at 20 wt% AEEP. The results suggest a formation of a nanocomposite, where amorphous starch/AEEP is the matrix, and amylopectin chains, mostly in their smectic conformation, as the reinforcing filler.
40 The obtained films displayed flexibility, strength, transparency and good thermal resistance. Also taken the biocompatibility of phosphazenes, these properties indicate that this new material warrants to be optimized for a new biodegradable plastic.

45

50
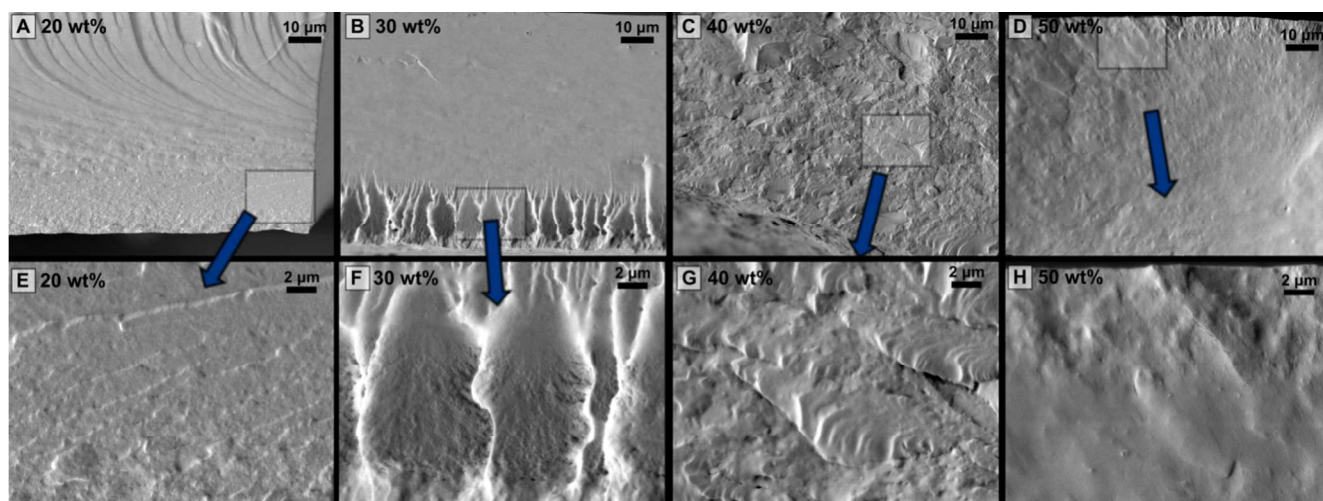
Fig. 8 The fracture surfaces for starch/AEEP for different AEEP-compositions imaged by scanning electron microscope

55

Acknowledgments

Notes and references

[a] *Molecular Materials, Department of Applied Physics, Aalto University School of Science, P.O. Box 15100, FI-00076 Aalto, Espoo, Finland.*

[b] *Current address: Instituto Nacional de Metrologia, Qualidade e Tecnologia Divisão de Materiais, 25.250-020, Duque de Caxias, Rio de Janeiro, Brazil.*

Eletronic Supplementary Information (ESI) available: Supporting information contains MS, ^{31}P NMR, all FTIR spectra, DSC and TGA curves as well as mechanical tests.

1 R. Parker, S. G. Ring, *J. Cereal Sci.*, 2001, **34**, 1.

2 A. Buléon, P. Colonna, V. Planchot, S. Ball, *Int. J. Biol. Macromol.*, 1998, **23**, 85.

3 A. Gandini, *Macromolecules*, 2008, **41**, 9491.

4 J-L. Jane, Structural Features of Starch Granules II. In *Starch - Chemistry and Technology*, ed. J. BeMiller and R. Whistler, Elsevier Academic Press: Amsterdam, 3rd edn., 2009; pp 193-227.

5 I. Damager, S. B. Engelsen, A. Blennow, B. Lindberg Møller, M. S. Motawia, *Chem. Rev.*, 2010, **110**, 2049.

6 L. Averous, P. J. Halley, *Biofuels, Bioprod. and Biorefin.*, 2009, **3**, 329.

7 Z. Wang, Z. Li, Z. Gu, Y. Hong, L. Cheng, *Carbohydr. Polym.*, 2012, **88**, 699.

8 O. V. López, C. J. Lecot, N. E. Zaritzky, M. A. García, *J. Food Eng.*, 2011, **105**, 254.

9 A. Serrero, S. Trombotto, Y. Bayon, P. Gravagna, S. Montanari, L. David, *Biomacromolecules*, 2011, **12**, 1556.

10 C. Johansson, J. Bras, I. Mondragon, P. Neehita, D. Packett, P. Simon, D. G. Svetec, S. Virtanen, M. G. Baschetti, C. Breen, F. Clegg, S. Aucejo, *Bioresources*, 2012, **7**, 2506.

11 A. Jiménez, M. J. Fabra, P. Talens, A. Chiralt, *Food Bioprocess Technol.*, 2012, **5**, 2058.

12 A. Gozzo, D. Glittenberg, Starch: A Versatile Product from Renewable Resourses for *Industrial Applications,* In *Sustainable Solutions for Modern Economies*; ed. R. Höfer, RSC Publ.: Cambridge, 2009, pp. 238-263.

13 D. Glittenberg, Starch-Based Biopolymers in Paper, Corrugated, and Other Industrial Applications, In *Polymer Science: A Comprehensive Reference,* ed. K. Matyjaszewski, M. Möller, Elsevier: Amsterdam, 2012, vol. 10 - Polymers for a Sustainable Environment and Green Energy, vol. ed. J. E. McGrath, M. A. Hickner, R. Höfner, pp. 165-193.

14 A. J. Salgado, O. P. Coutinho, R. L. Reis, J. E. Davies, *J. Biomed. Mater. Res., Part A*, 2007, **80A**, 983.

15 A. Rodrigues, M. Emeje, *Carbohydr. Polym.*, 2012, **87**, 987.

16 M. R.Vakili, N. Rahneshin, *Carbohydr. Polym.*, 2013, **98**, 1624.

17 F. G. Torres, S. Commeaux, O. P. Troncoso, *Starch - Stärke*, 2013, **65**, 543.

18 X. Liu, Y. Wang, L. Yu, Z. Tong, L. Chen, H. Liu, X. Li, *Starch - Stärke*, 2013, **65**, 48.

19 D. R. Daniels, A. M. Donald, *Macromolecules*, 2004, **37**, 1312.

20 J. Blazek, E. P. Gilbert, *Carbohydr. Polym.*, 2011, **85**, 281.

21 T. Witt, J. Doutch, E. P. Gilbert, R. G. Gilbert, *Biomacromolecules* 2012, **13**, 4273.

22 Y. Zhang, C. Rempel, Retrodegradation and Antiplasticization of Thermoplastic Starch, In *Thermoplastic Elastomers*, http://www.intechopen.com/books/thermoplastic-elastomers/retrodegradation-and-antiplasticization-of-thermoplastic-starch.ed. Sonbati, A. Z.El-, InTech, 2012, ch. 7, pp. 117-134.

23 M. Kaseem, K. Hamad, F. Deri, *Polym. Sci., Ser. A*, 2012, **54**, 165.

24 P. A. Perry, A. M. Donald, *Carbohydr. Polym.*, 2002, **49**, 155.

25 A. P. Mathew, A. Dufresne, *Biomacromolecules*, 2002, **3**, 1101.

26 P. Myllärinen, R. Partanen, J. Seppälä, P. Forssell, *Carbohydr. Polym.*, 2002, **50**, 355.

27 X. Ma, J. Yu, *Carbohydr. Polym.*, 2004, **57**, 197.

28 M. Huang, J. Yu, X. Ma, *Polym. Degrad. Stab.*, 2005, **90**, 501.

29 X. F.Ma, J. G.Yu, J. J. Wan, *Carbohydr. Polym.*, 2006, **64**, 267.

30 A. L. D. Róz, A. J. F. Carvalho, A. Gandini, A. A. S. Curvelo, *Carbohydr. Polym.*, 2006, **63**, 417.

31 P. S. Garcia, M. V. E. Grossmann, F. Yamashita, S. Mali, L. H. Dall'Antonia, W. J. Barreto, *Química Nova*, 2011, **34**, 1507.

32 H. Liu, F. Xie, L. Yu, L. Chen, L. Li, *Prog. Polym. Sci.*, 2009, **34**, 1348.

33 W. A. W. A. Rahman, L. T. Sin, A. R. Rahmat, A. A. Samad, *Carbohydr. Polym.*, 2004, **81**, 805.

34 M. Pizzoli, M. Scandola, Plasticizers, Polymer Plasticizer Interactions, In *Polymeric Materials Encyclopedia*, ed. J. C. Salamone, CRC Press: Boca Raton, 1996, vol. 7, pp. 5301-5307.

35 Huang, C.; Zhu, J.; Chen, L.; Li, L.; Li, X. *Food Control*, 2014, **36**, 55.

36 U. R. Halden, *Annu. Rev. Public Health*, 2010, **31**, 179.

37 A. M. Nafchi, M. Moradpour, M. Saiedi, A. K. Alias, *Starch/Stärke* 2013, **65**, 61.

38 P. A. Perry, A. M. Donald, *Biomacromolecules*, 2000, **1**, 424.

39 D. He, S. Y. Cho, D. W. Kim, C. Lee, Y. Kang, *Macromolecules* 2012, **45**, 7931.

40 H. R. Allcock, *Chemistry and Applications of Polyphophazenes*. John Wiley & Sons Ed: Hoboken, 2002.

41 R. Höfer, Processing and Performance Additives for Plastics, In *Polymer Science: A Comprehensive Reference*, ed. K. Matyjaszewski, M. Möller, Elsevier: Amsterdam, 2012, vol. 10 - Polymers for a Sustainable Environment and Green Energy, vol. ed. J. E. McGrath, M. A. Hickner, R. Höfner, pp. 369-381.

42 M. Gleria, R. De Jaeger, *J. Inorg. Organomet. Polym.*, 2001, **11**, 1.

43 M. Gleria, R. De Jaeger, Polyphosphazenes: A Review. In *New Aspects in Phosphorus Chemistry V,* ed. J-P. Majoral, Springer-Verlag Berlin: Berlin, 2005, vol. 250, pp. 165-251.

44 Y. S. Sohn, Y. J. Jun, Poly- and Cyclophosphazenes as Drug Carriers for Anticancer Therapy, In *Polyphosphazenes for Biomedical Applications,* ed. A. K. Andrianov, Jonh Wiley & Sons Inc.: New Jersey, 2009, pp. 249-276.

45 H. S. Wu, S. S. Meng, *Ind. Eng. Chem. Res.*, 1998, **37**, 675.

46 H. R. Allcock, A. Singh, A. M. A. Ambrosio, W. R. Laredo, *Biomacromolecules*, 2003, **4**, 1646.

47 A. Gabino Carriedo, J. I. Fidalgo Martínez, F. J. García Alonso, E. Rodicio González, A. Presa Soto, *Eur. J. Inorg. Chem.*, 2002, **2002**, 1502.

48 L. M. Frutos, G. A. Carriedo, M. P. Tarazona, E. Saiz, *Macromolecules*, 2009, **42**, 8769.

49 V. P. Silva Nykänen, M. A. Puska, A. Nykänen, J. Ruokolainen, *J. Polym. Sci., Part B: Polym. Phys.*, 2013, **51**, 1318.

50 D. Lourdin, H. Bizot, P. Colonna, *J. Appl. Polym. Sci.*, 1997, **63**, 1047.

51 J. J. G. van Soest, H. Tournois, D.de Wit, J. F. G. Vliegenthart, *Carbohydr. Res.*, 1995, **279**, 201.

52 I. Capron, P. Robert, P. Colonna, M. Brogly, V. Planchot, *Carbohydr. Polym.*, 2007, **68**, 249.

53 J. Doutch, E. P. Gilbert, *Carbohydr. Polym.*, 2013, **91**, 444.

54 T. A. Waigh, K. L. Kato, A. M. Donald, M. J. Gidley, C. J. Clarke, C. Riekel, *Starch/Stärke*, 2000, **52**, 450.

55 G. Liu, Y. Hong, Z. Gu, *Carbohydr. Polym.*, 2013, **98**, 995.

56 J. W. Donovan, *Biopolymers*, 1979, **18**, 263.

57 I. W. Hamley, *Soft Matter*, 2010, **6**, 1863.

58 Á. Kmetty, T. Bárány, J. Karger-Kocsis, *Prog. Polym. Sci.*, 2010, **35**, 1288.

59 C. Gao, L. Yu, H. N. Liu, L. N. Chen, *Prog. Polym. Sci.*, 2012, **37**, 767.

Green Chemistry Accepted Manuscript

60   A. B. Dias, C. M. O. Müller, F. D. S. Larotonda, J. B. Laurindo, *J. Cereal Sci.*, 2010, **51**, 213.

61   N. Laohakunjit, A. Noomhorm, *Starch/Stärke*, 2004, **56**, 348.

62   Y. Zhang, J. H. Han, *J. Food Sci.*, **2006**, 71, E253-E261.

63   L. Avérous, C. Fringant, L. Moro, *Polymer*, **2001**, 42, 6565-6572.

64   S. Gaudin, D. Lourdin, D. le Boltan, J. L. Ilari, P. Colonna, *J. Cereal Sci.*, 1999, **29**, 273-284.

65   J-L. Wang, F. Cheng, P-X. Zhu, *Carbohydr. Polym.*, 2014, **101**, 1109-1115.

66   X. F. Ma, J. G. Yu, N. Wang, *Carbohydr. Polym.*, 2007, **67**, 32-39.

67   L. Avérous, L. Moro, P. Dole, C. Fringant, *Polymer*, 2000, **41**, 4157.

68   P. Sarazin, G. Li, W. J. Orts,; B. D. Favis, *Polymer*, 2008, **49**, 599.

69   X. Tang, S. Alavi, *Carbohydr. Polym.*, 2011, **85**, 7.

70   J. Cheng, P. Zheng, F. Zhao, X. Ma, *Int. J. Biol. Macromol.*, 2013, **59**, 13-19.

This journal is © The Royal Society of Chemistry [year]
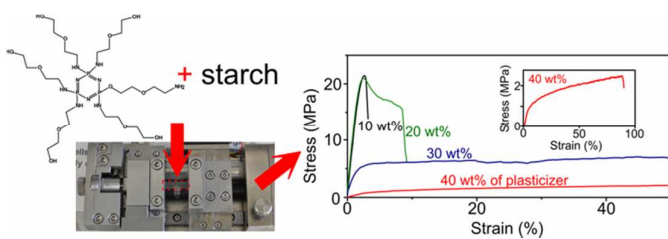
The combination of starch and a star-shaped non-hazardous plasticizer based on phosphazene produces self-reinforced composite films with temporal stability, no leaching and no retrodegradation.